Eratosthène

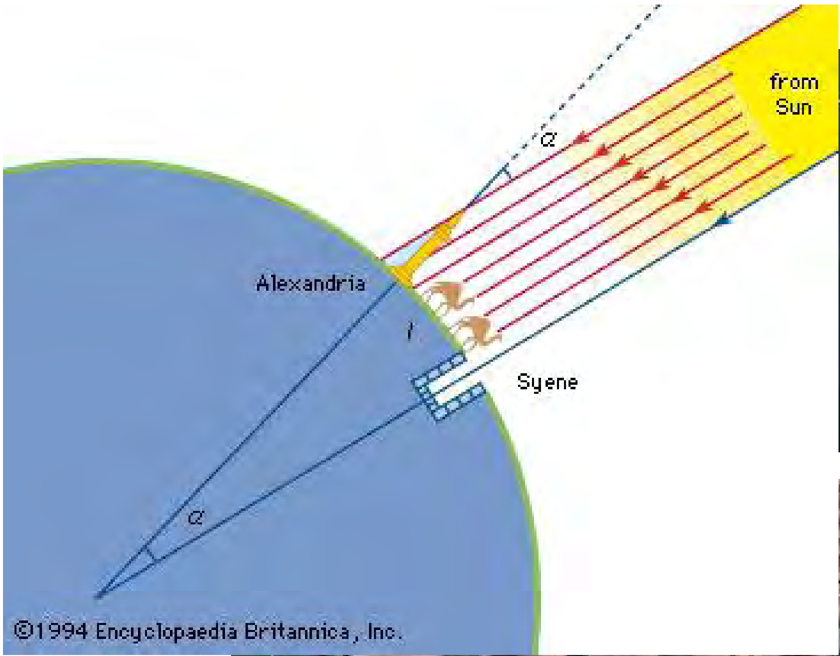

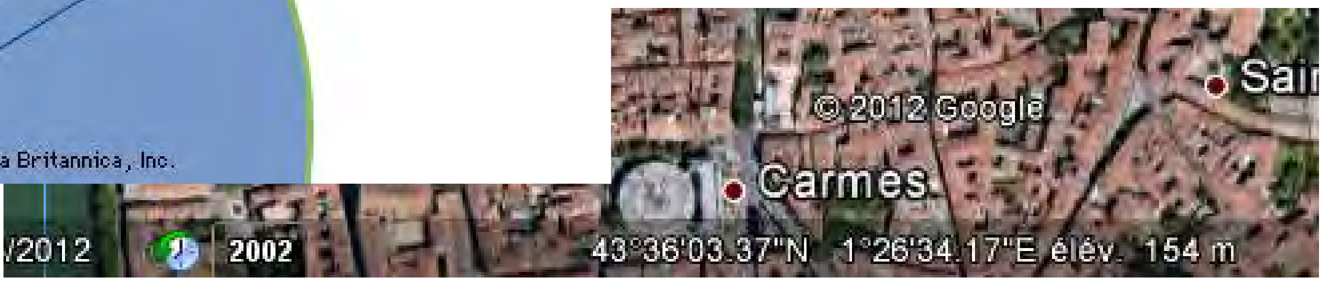

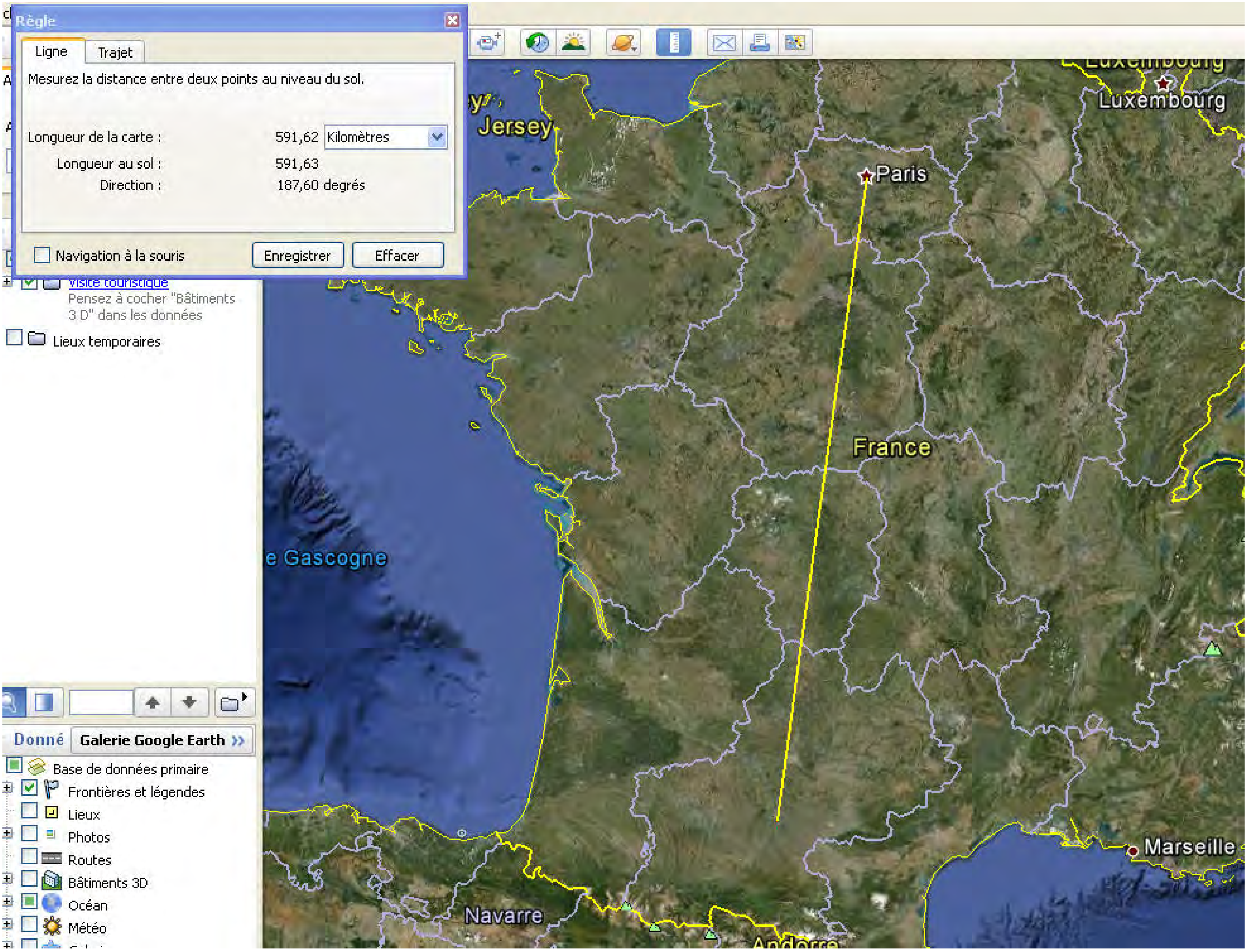

Distance Terre-Lune

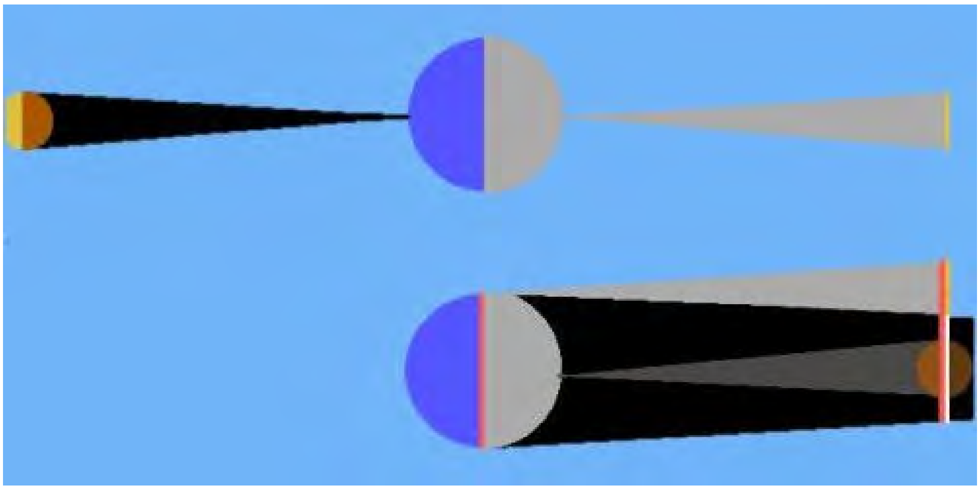

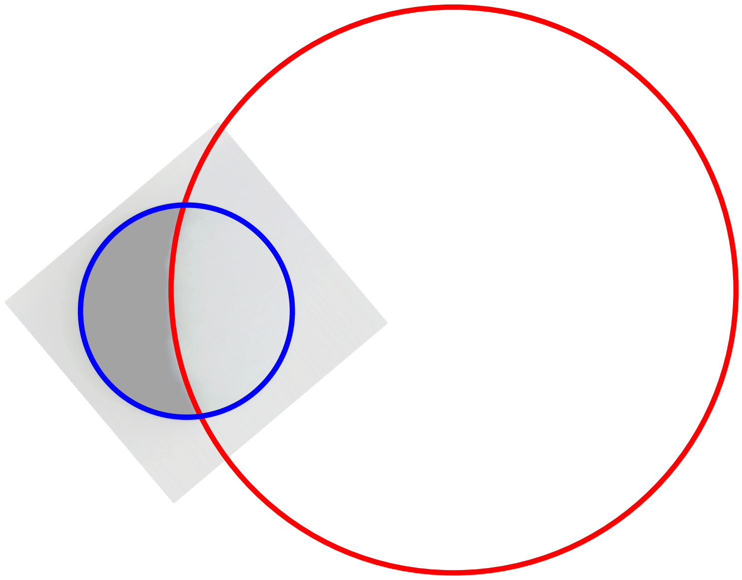

De la taille de la Lune et de sa taille apparente, on en déduit sa distance.

Le diamètre du cercle rouge est de 7,25 cm. Celui du cercle bleu est de 2,72 cm. À cette échelle, le diamètre de la Terre est de $7{,}25 + 2{,}72 = 9{,}97$ cm.

$$\varnothing\text{Lune} = \frac{2,72}{9,97} \times \overbrace{6,378\,10^{6}}^{\text{rayon équatorial de la Terre}} \times 2 = 3480072\,m$$

Le diamètre angulaire de la Lune varie entre $0,490^{0}$ et $0,558^{0}$. La valeur moyenne est donc de $0,524^{0}$.

$$d_L = \frac{3480072}{0,524 \times \dfrac{\pi}{180}} = 380\,000\,km$$

DRAW

STOP DRAW

CLEAR

1

Detected Frequency waves/second

Source Frequency waves/second

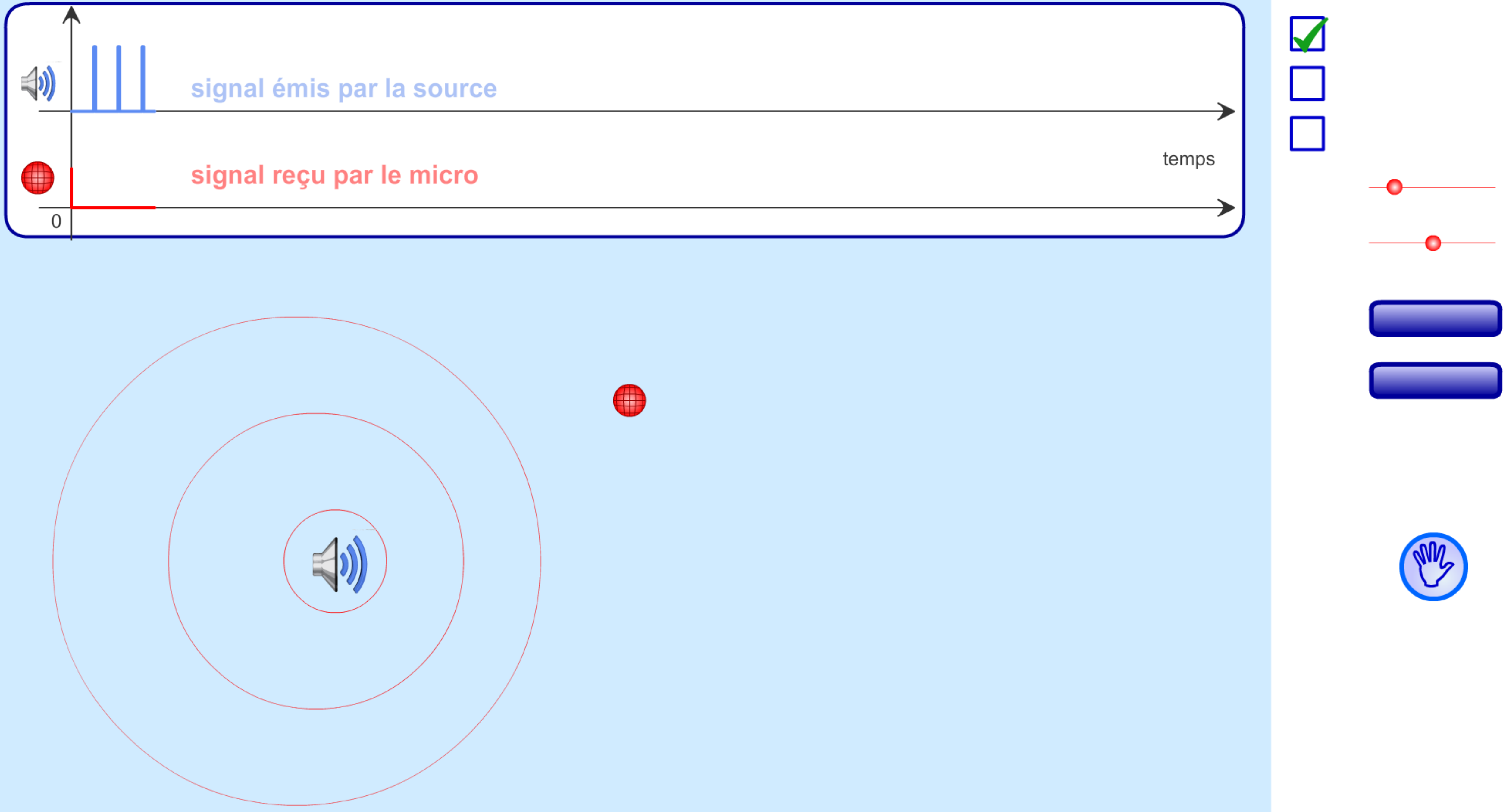

G.T.
09/12

EARTH'S ORBITAL VELOCITY

PROCEDURE

The plate scale (*dispersion*) of the spectrum of the the K giant star Arcturus can be found as shown in the figure below. Specifically, we must measure the distance *m* between the known reference lines of the spectrum of helium labelled "1" and "7" (see below).

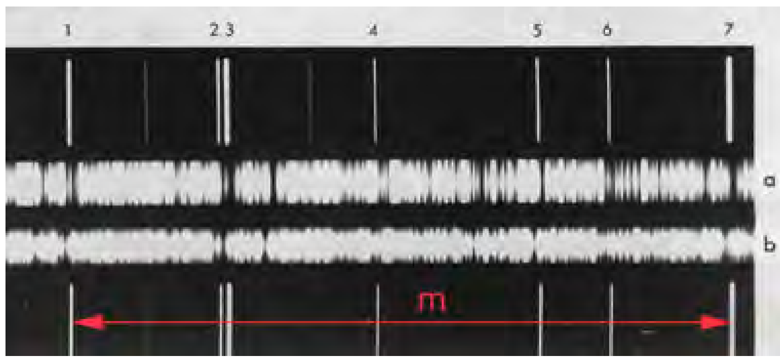

The dispersion is then

(4,307.91 Å – 4,260.48 Å) ÷ m = 47.43 Å ÷ 123.3 mm = 0.3847 Å/mm .

Now, looking at Spectrum a—the spectrum of Arcturus observed when the distance between the earth and the giant star increases (a redshift), we see that the same lines in the star's spectrum appear in the reference spectra above and below the star's absorption spectrum. The lines in Spectrum a are all uniformly shifted to the right of the reference lines. In addition, the spectrum of Arcturus observed when the distance between the star and Earth is decreasing (Spectrum b) also shows the same absorption lines albeit shifted to the left of the reference lines. Spectrum b therefore shows a blueshift.

Velocity Determinations

To determine the amount of the redshift and blueshift, we must choose a reference line and measure the position of the same line in Spectrum a and b from that reference line (see the example for line 5 shown in the figure below).

The Astronomical Unit is obtained by measuring the Doppler shift relative to the Earth of the narrow spectral features of galactic neutral hydrogen at 21 cm. The features chosen were the narrow absorption components in the spectra of Cassiopeia A, Taurus A and the emission at $l^{\mathrm{II}} = 0{\cdot}7^{\circ}$, $b^{\mathrm{II}} = 0{\cdot}0^{\circ}$. Observations which were taken over the period of one year gave two largely independent estimates of the Astronomical Unit which were combined to yield a value of 149 635 000 ± 19 000 (p.e.) km. This agrees with the value adopted by the IAU based on the radar value but it disagrees with the value determined optically by Rabe using a dynamical method.

Be careful to pay attention to the *sign* of your measurement because measurements to the right of the reference line (as found in Spectrum a) are considered to be *positive* while measurements of Spectrum b (to the left of the reference line) are considered to be *negative*. It is also absolutely critical to measure the shift of the spectral lines to the nearest 0.1 mm. Using our example for line 5, we find that

Shift of line 5 in Spectrum a = +0.8 mm

Shift of line 5 in Spectrum b = –1.0 mm .

Therefore, the actual shifts—found using the dispersion— are

$\Delta\lambda_a$ = +0.8 mm x 0.3847 Å/mm = +0.3078 Å

$\Delta\lambda_b$ = –1.0 mm x 0.3847 Å/mm = –0.3847 Å .

Next, the Doppler velocity equation given on the back page of the lab handout

$v = c\Delta\lambda/\lambda o$,

can be used to calculate the redshifted and the blueshifted velocities of line 5:

V_A = 300,000 km/s x (+0.3078Å) ÷ 4,294.13 Å = +21.50 km/s

V_B = 300,000 km/s x (–0.3847 Å) ÷ 4,294.13 Å = –26.88 km/s .

Now, the orbital velocity of Earth is calculated using equation (1) to be

$V_o = ½(V_A - V_B)$ = 0.5 x (+21.50 km/s – (–26.88 km/s)) = +24.19 km/s

while the radial (line-of-sight) velocity of Arcturus is found to be

$V_s = ½(V_A + V_B)$ = 0.5 x (+21.50 km/s + (–26.88 km/s)) = –2.690 km/s .

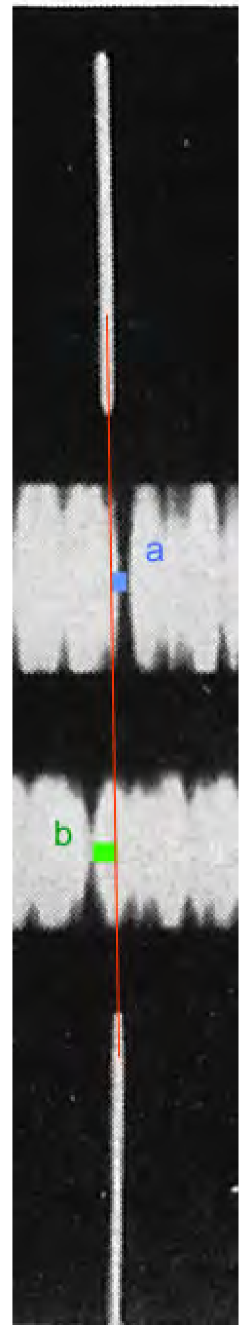

Results

Arcturus does not lie exactly on the earth's orbital plane, however, so we must make a minor correction to the orbital velocity of Earth to account for Arcturus' declination. Given that the star is 30.8° above the ecliptic, we must correct our calculation of the earth's orbital velocity by a factor of cos 30.8°. Therefore, the corrected orbital velocity of Earth is V_c = +24.19 km/s ÷ cos 30.8° = +24.19 km.s ÷ 0.86 = 28.13 km/s .

In order to ensure the most accurate measurement of the orbital velocity, the entire set of calculations should be repeated for two other spectral line pairs and the three orbital velocities averaged.

Finally, the radius of the earth's orbit can be determined simply by using the average orbital velocity and knowing the orbital period (in other words, the number of seconds in one year). Using the relationship between velocity and the orbital period, we have circular velocity = circumference of circle ÷ orbital period .

With our data,

$V_c = 2\pi R \div P$

or, solving for the earth's orbital radius

$R = V_c P \div 2\pi$ = 28.13 km/s x 31,560,000 s ÷ (2 x 3.14159) = 141,300,000 km

where P is simply the earth's orbital period expressed as the number of seconds in one year.

Given that the accepted value for the semimajor axis of Earth's orbit is 149,600,000 km, our calculation has an error of 5.6% .

Parallax

Definition

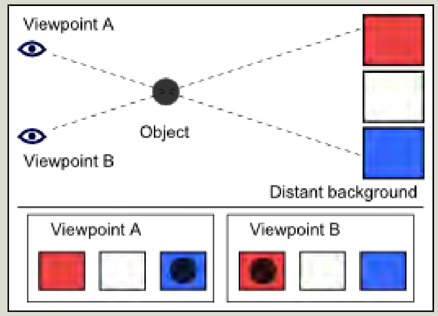

A simple example of parallax.

Parallax is the apparent shift of an object's position relative to more distant background objects caused by a change in the observer's position. In other words, parallax is a perspective effect of *geometry*. It is the observed location of one object with respect to another – nothing more.

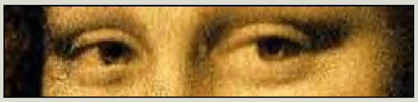

Humans are already very accustomed to parallax as our two eyes provide a small parallax effect known as stereo vision. The left eye has a slightly different point of view than the right eye. This can easily be seen by looking at the location of a nearby object relative to more distant objects first throught one eye alone and then through the other eye. The brain uses the two images to create *depth perception* (along with several other clues). The parallax contribution to depth perception only works for close objects. When an object is far away, the shift in position of a foreground object to the even more distant background becomes too small for the eyes and brain to register.

Parallax of Stars

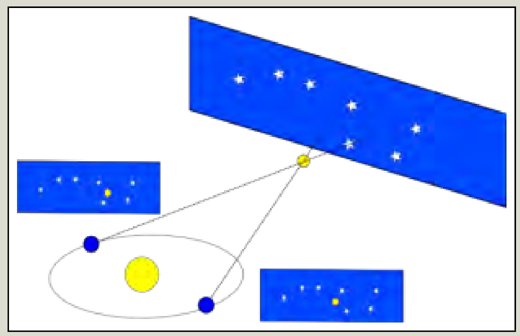

Parallax with a 2 A.U. baseline.

Stars are very far away – yet some stars are closer than others. Do these closer stars exhibit parallax? The answer turns out to be yes, but the parallax is very small – far smaller than can be seen with the naked eye. The first successful measurements of a stellar parallax were made by Friedrich Bessel in 1838, for the star 61 Cygni.

To create the largest parallax effect, we need to have the largest shift in position for the observer. The largest shift possible from the Earth is 2 AU – the diameter of the Earth's orbit. This shift corresponds to two positions of the Earth 6 months apart. Assuming the star being observed doesn’t move much in 6 months (a very good assumption), an astronomer need only look at its position once, wait 6 months and measure the position again relative to the much more distance stars.

1 parsec is defined as the distance when a baseline of 1 AU subtends a parallactic angle of 1 arcsecond.

Because the parallactic baseline would be given in astronomical units, astronomers also defined a distance in terms of that baseline known as the *parsec*. It is defined as the the distance at which a baseline of 1 AU subtends a parallactic angle of 1 arcsecond (1/3600th of a degree).

The diagram below allows one to explore how parsec is calculated. It is nothing more than basic trigonometry. Note that the diagram is not to scale. The real triangle is much, much longer (it is over 200,000 times longer than it is tall).

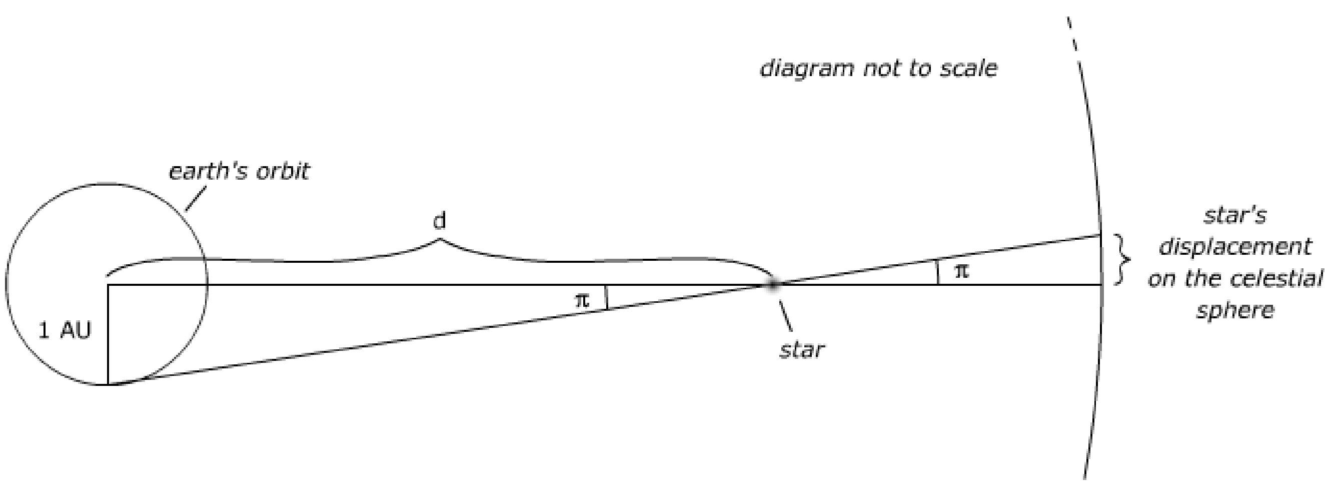

$$d = \frac{1}{\pi''} = \frac{1}{\boxed{1}\,''} = \boxed{1}\ \text{pc} = \boxed{3.26}\ \text{ly}$$

π measured in arcseconds (")

1 parsec (pc) = 3.26 lightyears (ly)

Determining distances through the moving cluster method

There is another method that can help confirm the results of the parallax method. (This method is not included in our book, but it is quite ingenious.) It works for stars that are further away if they are in a cluster. It is necessary to suppose that the stars are all moving together. This is is based on the idea that the stars in the cluster all came from the same gas cloud.

This method has been successfully applied to (just) one cluster, the Hyades (the head of Taurus the Bull), which is found to be 40 pc away.

To understand the method, we need to proceed step by step. We consider first one star in the cluster. Let *d* be the distance to the star in pc. We don't know *d*. We want to know it.

From photographs taken, say, 10 years apart, we can see that the star has moved. (It has *proper motion*.) Let us suppose that the proper motion is 3 arc sec in ten years.

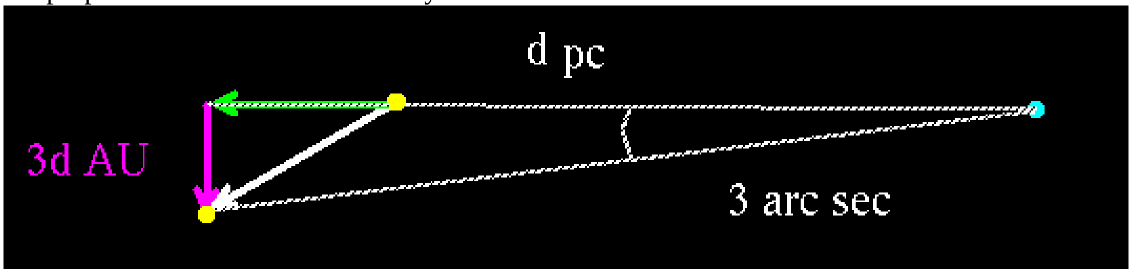

We can conclude that the star has moved 3 times *d* astronomical units across our line of sight. (But we don't know *d*).

From measurments of the doppler shift of light from our star, we can determine how fast it is moving toward us or away from us. Let us suppose that the speed is 2 AU per year away from us, so that in the ten years it has moved 20 AU further away:

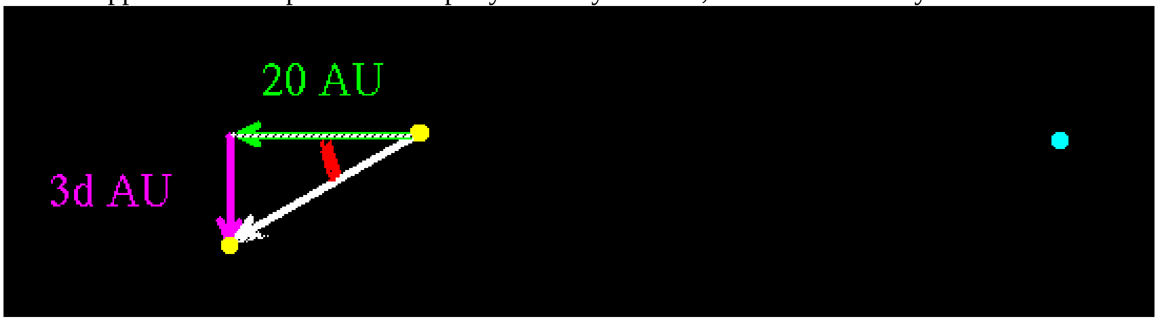

Now if we knew the direction in which the star is moving, we could determine *d*.

How can we determine the direction of motion? Here is where the cluster comes in. Our star is in a cluster and they are all moving in the same direction. (That is, we have to assume that they are all moving in the same direction.).

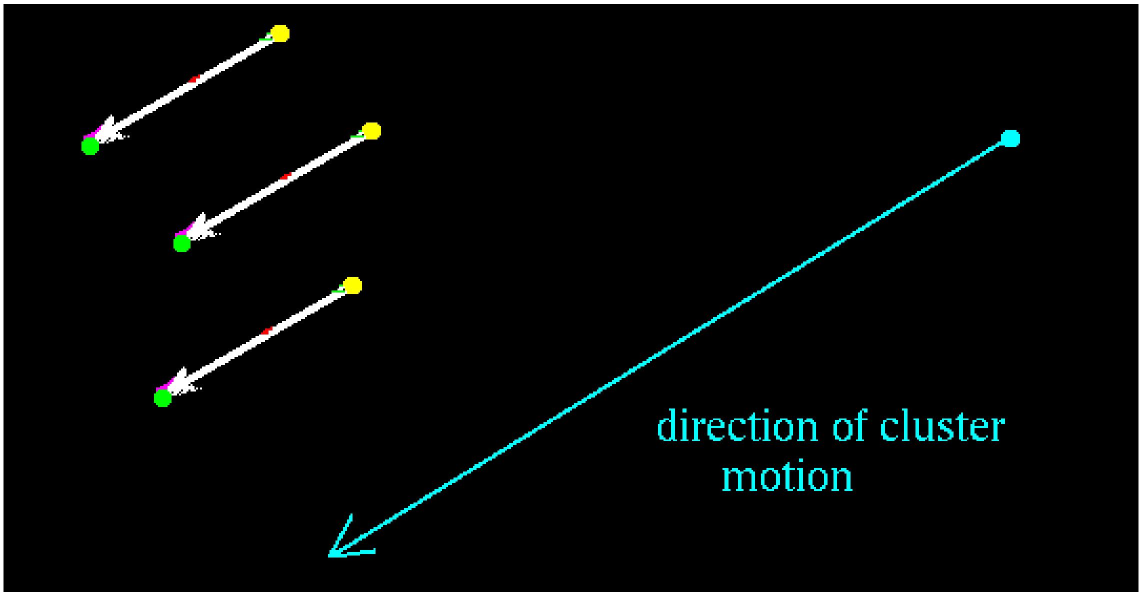

If there were some way that we could determine the direction in which the cluster is moving, we would be done!

The art of finding the direction of the cluster

Here is a famous surrealistic painting by Magritte. It may be surrealistic, but part of it is realistic. That has to do with how parallel lines in three dimensional space look when represented on a two dimensional canvas. Here is what Magritte did.

All artists know this, and astronomers know it too. From our two photographs of the star cluster taken 10 years apart, we can plot the directions that the stars are moving as seen on the ``canvas'' of the sky.

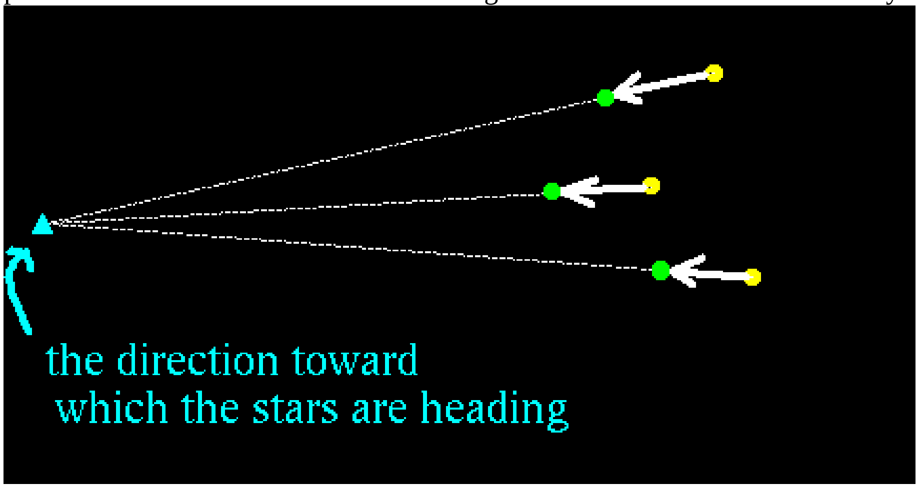

Since the paths of the stars are parallel lines, they seem to converge on a *vanishing point*. The direction from Earth to the vanishing point is the direction of motion of the cluster.

We use the direction of motion that we now know to determine the distance to the stars in the cluster.

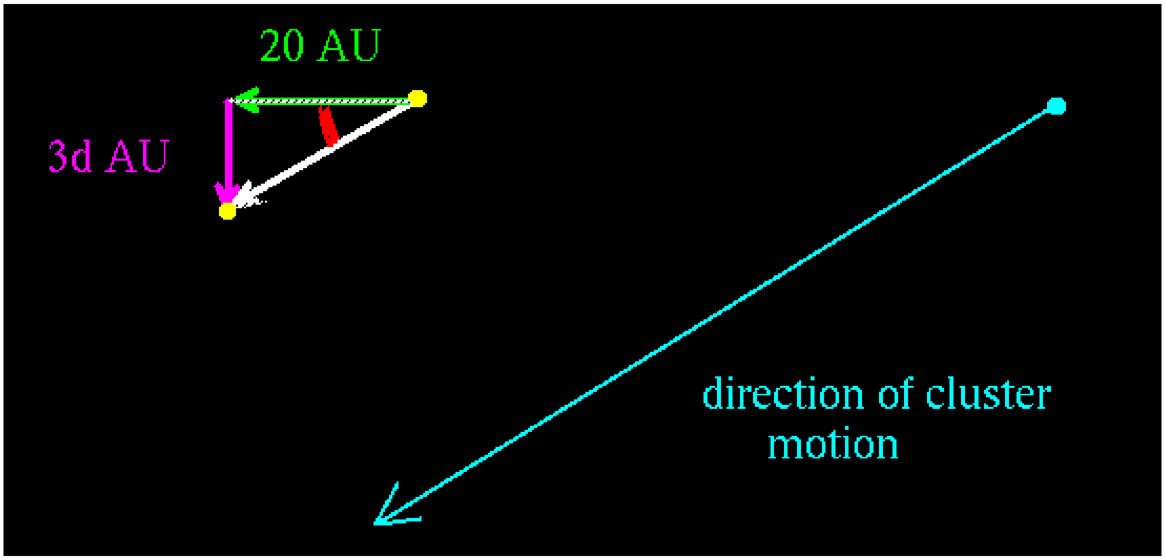

Astronomers use trigonometry, but you could just make a scale drawing to determine the length of the purple line in AU. Dividing this length by 3 in our example gives the distance to the cluster in parsecs.

[ASTR 122 course home page]

Updated 22 Octobber 2007

Davison E. Soper, Institute of Theoretical Science, University of Oregon, Eugene OR 97403 USA

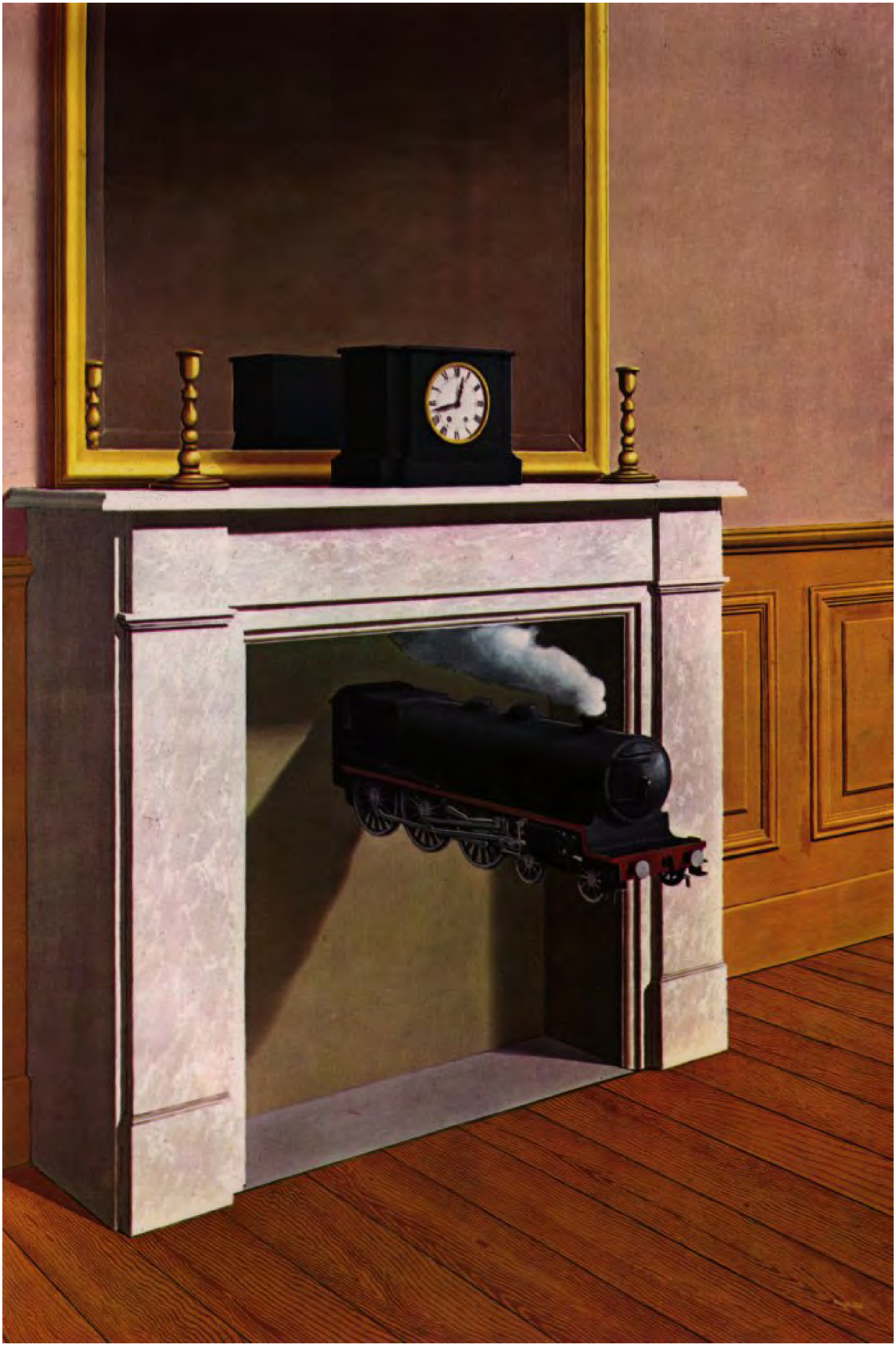

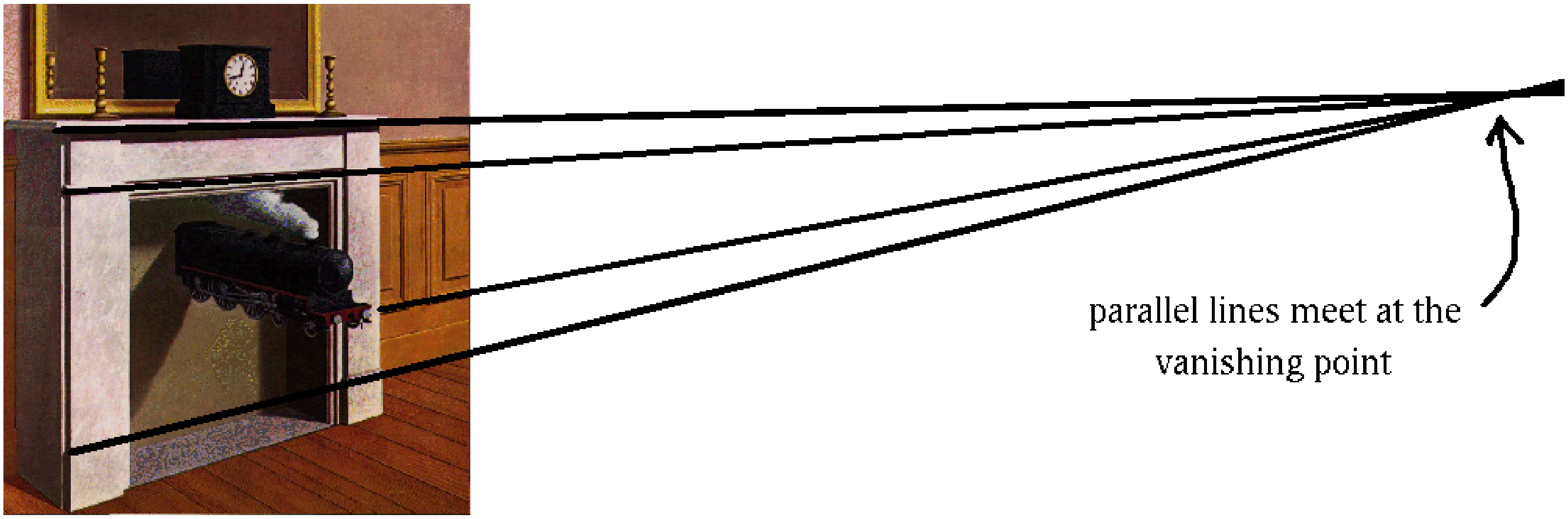

L'amas des Hyades est à 133 années lumières. Il permet d'étalonner le diagramme d'Hertzsprung-Russel. Une fois ce diagramme étalonné, il permet de calculer les distances de 6 amas ouverts.

On trouve dans ces 6 amas ouverts 9 céphéides,et ces 6 amas ouverts de distances connues permettent d'étalonner la relation période-luminosité pour ces 9 céphéides.

Les céphéides sont des supergéantes rouges venant d'étoiles de masses comprises entre 2 et 10 masses solaires dans lesquelles l'hélium s'allume tranquillement. Ces étoiles pulsent car elles fonctionnent comme des machines thermodynamiques. Dans les couches périphériques, le gaz est à la limite entre être ionisé et être neutre. Il reçoit de l'énergie quand il est ionisé (piège les photons) car chaud, sous haute pression, et perd de l'énergie quand il est neutre (laisse passer les photons) car froid, sous basse pression. Cette zone limite entre une surface neutre et ionisée correspond à la zone d'instabilité du diagramme d'Hertzsprung-Russel où sont les Céphéides et les RR Lyrae.

Un autre type d'étoiles pulsantes, pour la même raison, sont les supergéantes venant d'étoiles de masses entre 0,7 et 2 masses solaires où l'hélium s'allume quand il est dégénéré provoquant le flash de l'hélium. Ce sont les RR Lyrae.

Lorsque l'étoile a au départ une masse supérieure à 10 masses solaires, elle finit sa vie en explosant, formant ce qu'on appelle une supernova

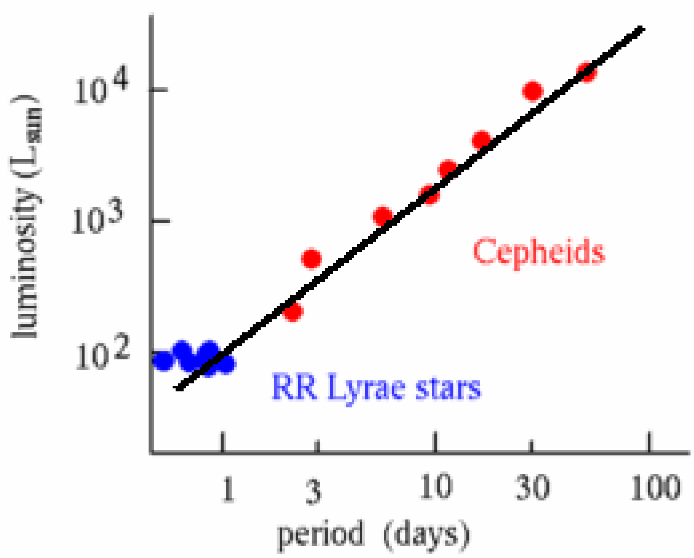

Une dans :	$NGC6087$
1	$NGC129$
1	$M25$
1	$NGC7790$
1	$NGC6664$
4	$h + \chi\ Persei$

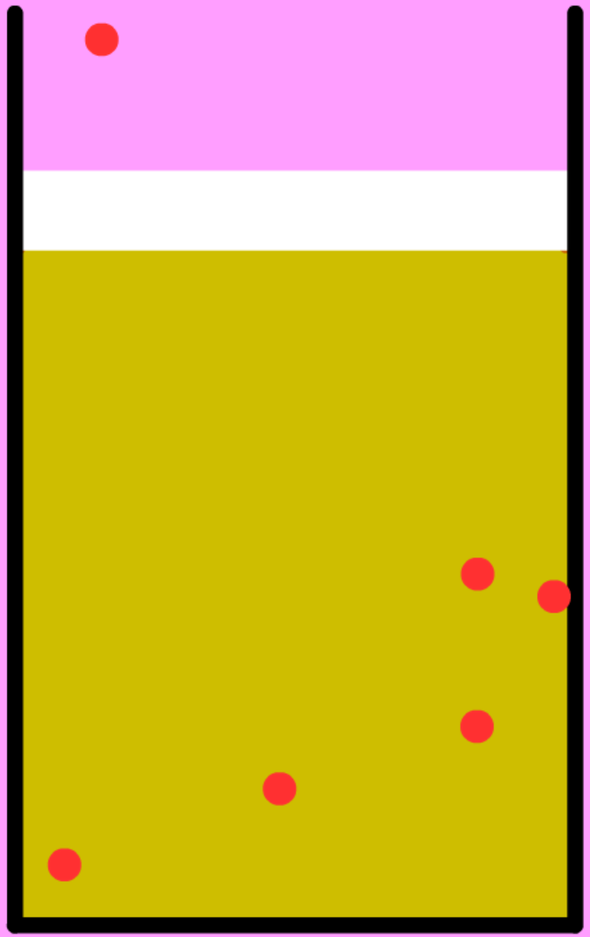

Le système est à capacité thermique négative à cause du théorème du viriel qui dit que l'énergie cinétique est opposée à l'énergie totale. Quand le système reçoit de l'énergie, il se refroidit et quand il perd de l'énergie il se réchauffe.

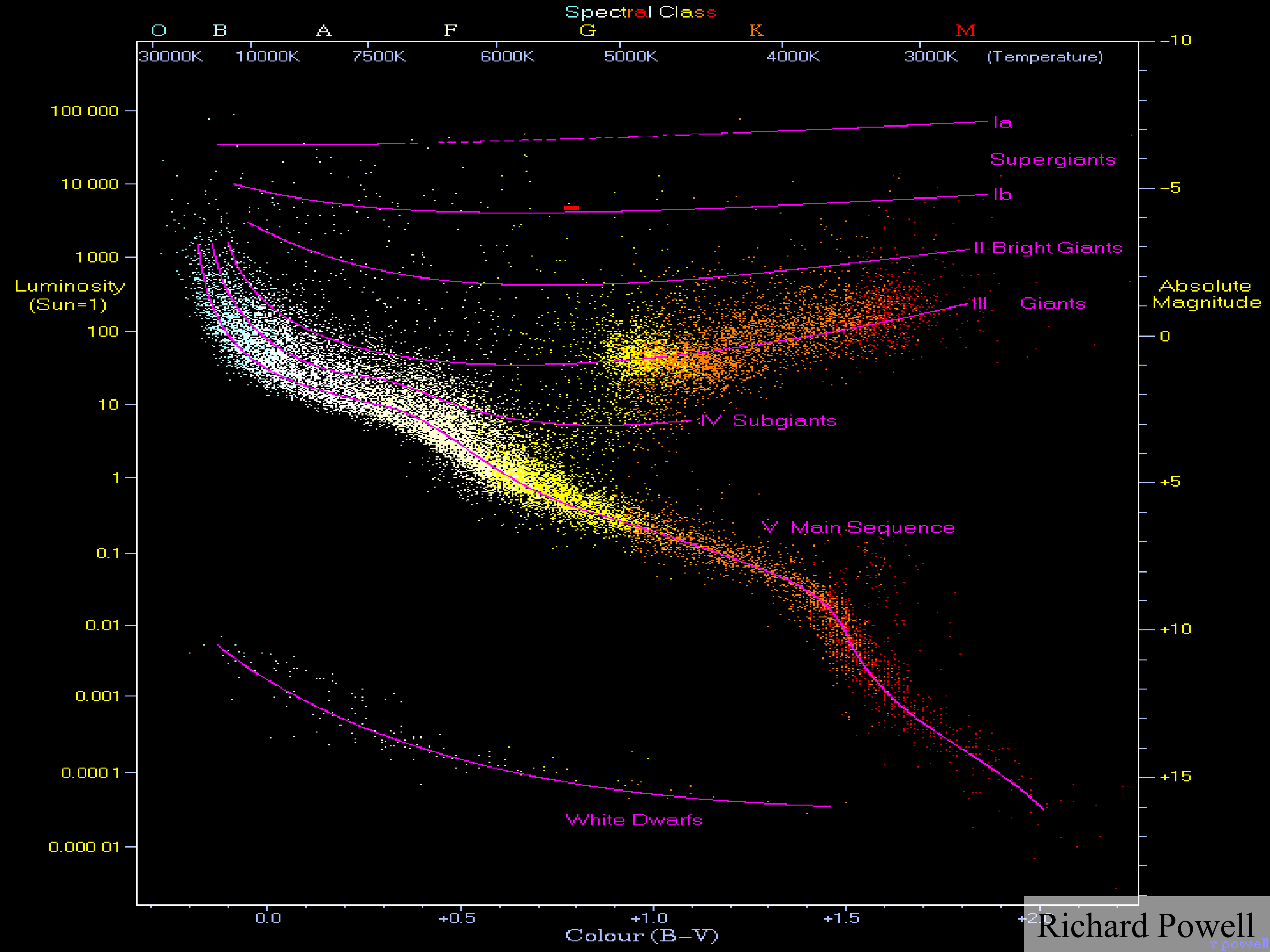

Spectral Class
O B A F G K M
30000K 10000K 7500K 6000K 5000K 4000K 3000K (Temperature)
Luminosity (Sun=1)
100 000
10 000
1 000
100
10
1
0.1
0.01
0.001
0.0001
0.000 01
Absolute Magnitude
−10
−5
0
+5
+10
+15
Ia
Supergiants
Ib
II Bright Giants
III Giants
IV Subgiants
V Main Sequence
White Dwarfs
0.0
+0.5
+1.0
+1.5
+2.0
Colour (B−V)
Richard Powell

Astronomy 12 - Spring 1999 (S.T. Myers)

The Tully-Fisher and Faber-Jackson Relations

There are 3 "observable" physical properties of galaxies, R, L, and M, as there are in stars. These are given by the relations

$$\theta = \frac{R}{d}$$
$$f = \frac{L}{4\pi d^2}$$
$$v^2 = \frac{GM}{R}$$

The distance *d* enters into the small-angle relation and the flux-luminosity relation. We can eliminate this between the two using the surface brightness

$$I = \frac{f}{\theta^2} = \frac{Lv^4}{4\pi G^2 M^2}$$

which is independent of the distance, as we discussed in Lecture 3. We can rearrange this to find

$$L = \frac{v^4}{I} \frac{1}{4\pi G^2 (M/L)^2}$$

where we have introduced the mass-to-light ratio *M*/*L*. If we can assume that for a given class of galaxies that the central surface brightness I (in Lsun/pc^2) and the mass-to-light ratio *M*/*L are constant*, then we find the relation

$$L \propto v^4$$

which is the basis of some of the most useful distance indicators in cosmology! For instance, if we are observing spiral galaxies, the appropriate velocity to use is the maximum velocity *v_max* in the rotation curve which can be determined from H I spectra. Then, we have

$$L \propto v_{max}^4$$

which is known as the **Tully-Fisher relation**. On the other hand, if we are concerned with elliptical galaxies, the appropriate velocity is the central *velocity dispersion*

$$L \propto \sigma_v^4$$

which is known as the **Faber-Jackson relation**. Both of these relations were discovered empirically and are justified through the arguments given above. The proportionality must be calibrated using galaxies with known distances, then the relations can be used to find the luminosity, and thus the distance, given an observation of the apparent magnitude and velocity width. For example, a typical relation for ellipticals is

$$\log \sigma_v = -0.1\, M_B + 0.2$$

where M_B is the absolute galaxy magnitude (to some isophotal level) in the B band.

Note that it is still under debate whether these relations are *universal*, that is, whether I and M/L are dependent only on the galaxy type, and do not depend on other things such as location and environment.

Astro12 Index --- Astro12 Home

---

smyers@nrao.edu Steven T. Myers

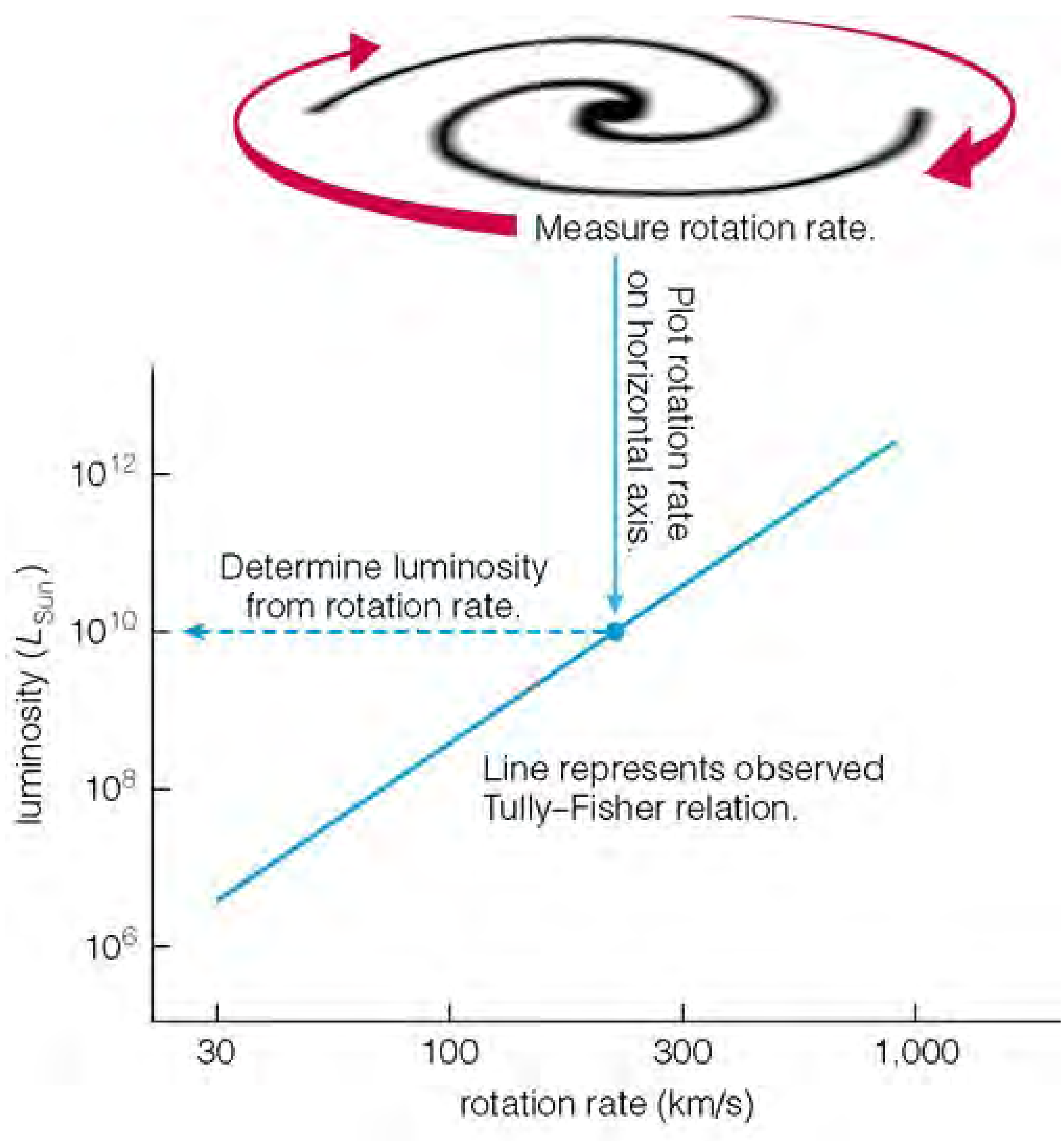

The Cosmic Distance Scale

A very important task in modern astronomy is the measurement of distances to things that are very far away. We have seen earlier some methods for [measuring distances] to relatively nearby objects.

The Measurement of Distances: Standard Candles

At very large distances such as those to galaxies beyond the local group or the local supergroup, astronomers can no longer use the methods such as trigonometric parallax or Cepheid variables that we have discussed before because the parallax shift becomes too small, and because at sufficiently large distances we can no longer even see individual stars in galaxies.

At those distances, astronomers turn to a series of methods that use *standard candles:* objects whose absolute magnitude is thought to be very well known. Then, by comparing the relative intensity of light observed from the object with that expected based on its assumed absolute magnitude, the [inverse square law] for light intensity can be used to infer the distance.

Example of a Standard Candle: Type Ia Supernovae

One example of a standard candle is a type Ia supernova. Astronomers have reason to believe that the peak light output from such a supernova is always approximately equivalent to an absolute blue sensitive magnitude of -19.6. Thus, if we observe a type Ia supernova in a distant galaxy and measure the peak light output, we can use the inverse square law to infer its distance and therefore the distance of its parent galaxy.

Because type Ia supernovae are so bright, it is possible to see them at very large distances. Cepheid variables, which are supergiant stars, can be seen at distances out to about 10-20 Mpc; supernovae are about 14 magnitudes brighter than Cepheid variables, which means that they can be seen about 500 times further away. Thus, type 1a supernovae can measure distances out to around 1000 Mpc, which is a significant fraction of the radius of the known Universe.

A Comparison of Methods for the Virgo Cluster

The following table lists a variety of methods for determining large distances as applied to the same problem: determining the distance to the Virgo Cluster of galaxies.

Distance Methods Applied to the Virgo Cluster

Method	Uncertainty (Mag)	Distance (Mpc)	Uncertainty (Mpc)	Range (Mpc)
Cepheids	0.16	14.9	1.2	20
Novae	0.40	21.1	3.9	20
Plan. Nebulae	0.16	15.4	1.1	30
Glob. Clusters	0.40	18.8	3.8	50
S. Bright. Fluct.	0.16	15.9	0.9	50
Tulley-Fisher	0.28	15.8	1.5	>100
D-Sigma	0.50	16.8	2.4	>100

Supernova (1a)	0.53	19.4	5.0	>1000

Source: *An Introduction to Modern Astrophysics*, B. W. Carrol and D. A. Ostlie (Addison-Wesley, 1996)

We shall not discuss the details of how all these methods work, but we note that there is reasonably good agreement on the distance to the Virgo Cluster (the average among the different techniques is approximately 15 Mpc). This gives us some confidence that these methods can be used to measure large distances. The last column (Range) gives the largest distance at which these methods can be used. We see that distances in excess of 1000 Mpc may be measured.

Next Back Top Home Help

DISTANCES PLUS LOINTAINES

L'étape suivante est de déterminer la distance de la galaxie la plus proche de nous, la galaxie d'Andromède. Ceci est fait grâce aux céphéides. On a leurs éclats apparents, et leurs éclats réels avec leurs périodes, on en déduit leurs distances. La distance de la galaxie d'Andromède M31 est de 2,2 millions d'années lumières.

Ensuite on en déduit la distance de l'amas de galaxies de la Vierge en supposant que l'amas globulaire le plus brillant de M87 a la même luminosité absolue que le plus brillant amas globulaire de M31 : B282. La galaxie M87 est énorme avec beaucoup d'amas globulaires et un énorme trou noir au centre qui émet un jet puissant. C'est une galaxie elliptique. L'amas de la Vierge est à 50 millions d'années lumières. Ce sont les galaxies les plus lointaines que l'on peut voir avec un 200 mm d'ouverture.

La distance aux amas de galaxies plus lointains est déterminée en supposant que leur plus brillante galaxie *E* a la même luminosité absolue que la plus brillante galaxie de l'amas de la Vierge, NGC4472.

Une autre technique est la relation de Tully-Fisher qui dit que la luminosité absolue d'une galaxie est proportionnelle au carré de la vitesse maximale de ses constituants, vitesse déterminée par effet Doppler.

Un autre étalon qui permet de mesurer les distances très lointaines est constitué des supernovae de type Ia. Les supernovae de type Ia n'ont pas de raies de l'hydrogène dans leur spectre. Il s'agit de naines blanches qui avalent par effet de marée la matière d'une géante rouge qui tourne autour d'elle. Lorsque la masse dépasse la masse limite de Chandrasekhar de 1,46 masse solaires, les électrons dégénérés (leur vitesse n'est pas due à la température mais à la mécanique quantique) devenant relativistes ne peuvent plus augmenter de vitesse pour soutenir l'étoile qui s'effondre en étoile à neutron. Ce faisant l'hydrogène est avalé et chauffé et fusionne brutalement en hélium, et tout se termine dans une gigantesque explosion qui ne laisse aucune cendre.

L'étoile disparaît complétement. Les naines blanches ayant toutes la même composition et la même masse quand elles explosent, les supernovae de type Ia on toutes exactement la même luminosité absolue et peuvent servir d'étalons de distances.

$d_L = \frac{C}{H0}\left(z + \frac{1}{2}(1 - q_0)\, z^2 + \ldots\right)$ où d_L est la distance lumineuse, distance réelle pour un univers plat où l'énergie lumineuse se répartit dans le volume 4/3 π R^3. q_0 est le paramètre de décélération et vaut – S S''/(S')^2 , *S* étant l'échelle de l'univers. Si l'expansion de l'univers s'accélère, q_0 négatif et la distance lumineuse est plus grande que prévue pour un décalage vers le rouge donné, ou le décalage vers le rouge est moins grand que prévu pour une distance lumineuse donnée (affaiblissement de la lumière donné, donc différence entre magnitude absolue et apparente donnée). Ceci est évident, en effet si l'expansion de l'univers s'accélère, lorsque l'objet a émis la lumière qui nous atteint, il nous fuyait avec une vitesse moins grande que prévue, compte tenue de la valeur actuelle de la constante de Hubble H_0, donc il a un décalage vers le rouge plus faible. Tel est le cas. Ce serait l'énergie sombre qui aurait une pression négative donc un effet gravitationnel répulsif qui agirait. Elle serait liée à l'énergie de point *0* du vide.

Rappelons que le décalage vers le rouge *z* est défini par : z = Δ γ/γ . Il vaut :

$$z = \sqrt{\frac{1 + v/C}{1 - v/C}} - 1$$

quand $v \ll C$ $z = v/C$ comme en Mécanique newtonienne.

Quand $v \rightarrow C$ $z \rightarrow \infty$.

Que se passe-t-il aux distances cosmologiques ?

$z > 0{,}3 \quad \text{ou} \quad d > 1250\,\text{Mpc}$

$1250\,\text{Mpc} \simeq 4 \cdot 10^{9}\,\text{al}$

- Le signal qui nous parvient représente l'état de la source il y a **4 Milliards d'années** !
- Pendant le trajet de la lumière, **l'univers s'est dilaté**
- **Le temps et l'espace sont liés** en raison de la vitesse finie de la lumière
- Une interprétation **relativiste** est nécessaire (Einstein, 1913)

Hypothèse cosmologique faible : univers isotrope en tout point

$$ds^2 = c^2\, dt^2 - a^2(t) \left[\frac{dr^2}{1 - k\, r^2} + r^2\, d\theta^2 + r^2\, \sin^2\theta\, d\varphi^2 \right]$$

Les supernova type Ia

L'explosion thermonucléaire se déclenche lorsque la **masse de Chandrasekar** (≅ 1,4 M) est atteinte.

Pour toutes les SN Ia, la même masse explose de la même manière ⇒ **même luminosité**

La supernova SN 1994D et la galaxie NGC4526

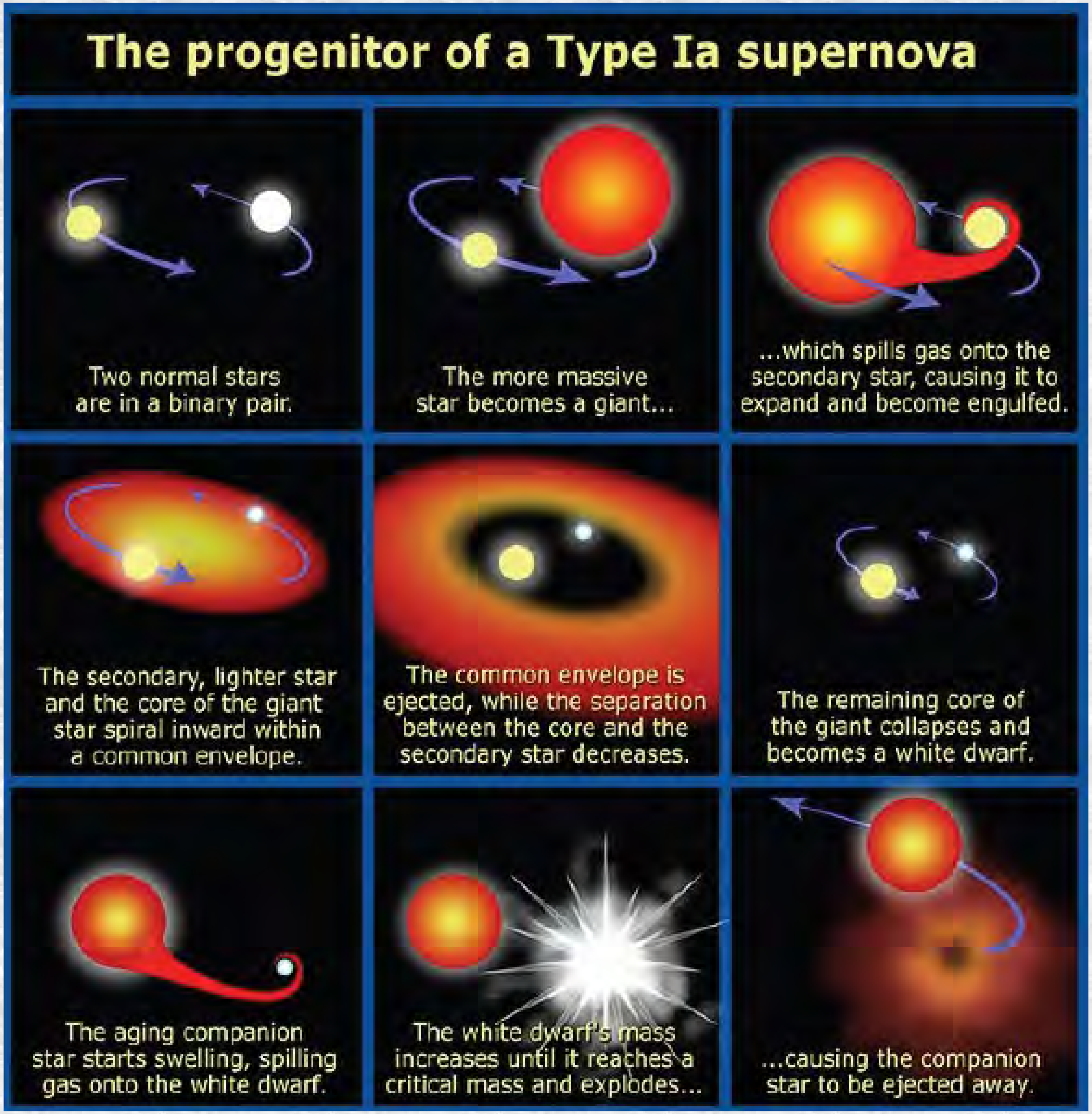

Estimation des paramètres cosmologiques à partir des SN Ia

La distance d_L mesurée par les SN Ia dépend des paramètres cosmologiques !

$$d_L = \frac{1+z}{H_0\sqrt{|\Omega_k|}} S\left(c\sqrt{|\Omega_k|} \int_0^z \frac{dz'}{\sqrt{\Omega_M(1+z')^3 + \Omega_k(1+z')^2 + \Omega_\Lambda}} \right)$$

$$S(u)=\sin u \quad \text{si} \quad \Omega_k<0 \qquad S(u)=u \quad \text{si} \quad \Omega_k=0 \qquad S(u)=\sinh u \quad \text{si} \quad \Omega_k>0$$

Si z est suffisamment petit :

$$d_L = \frac{c}{H_0} z \left[1 + \frac{z}{2}(1-q_0) + O(z^2) \right]$$

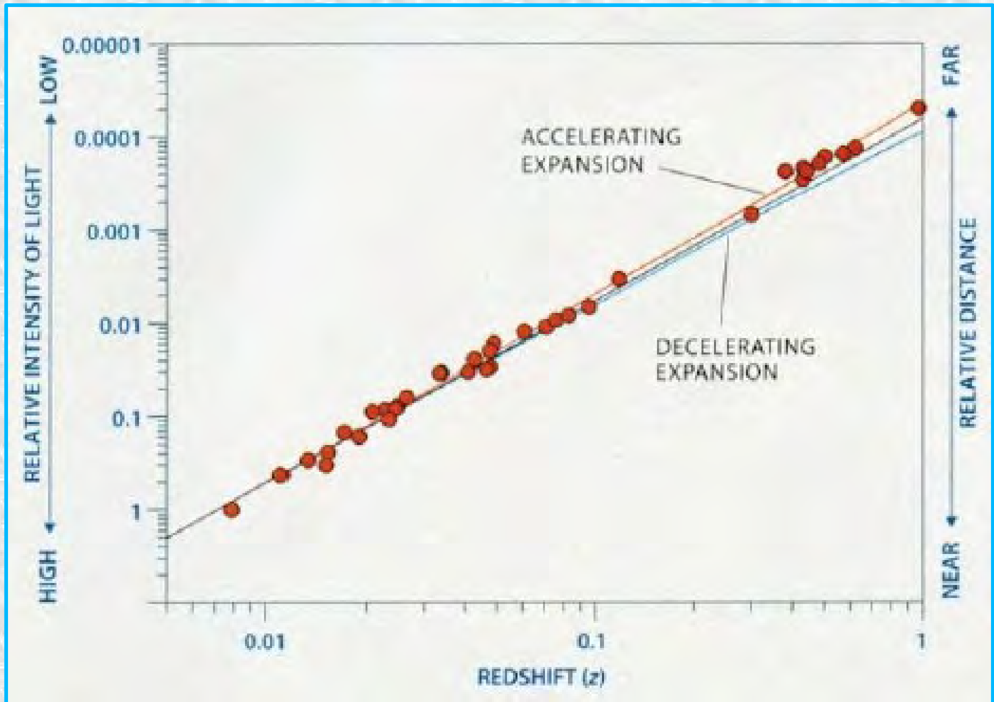

L'expansion de l'univers s'accélère !

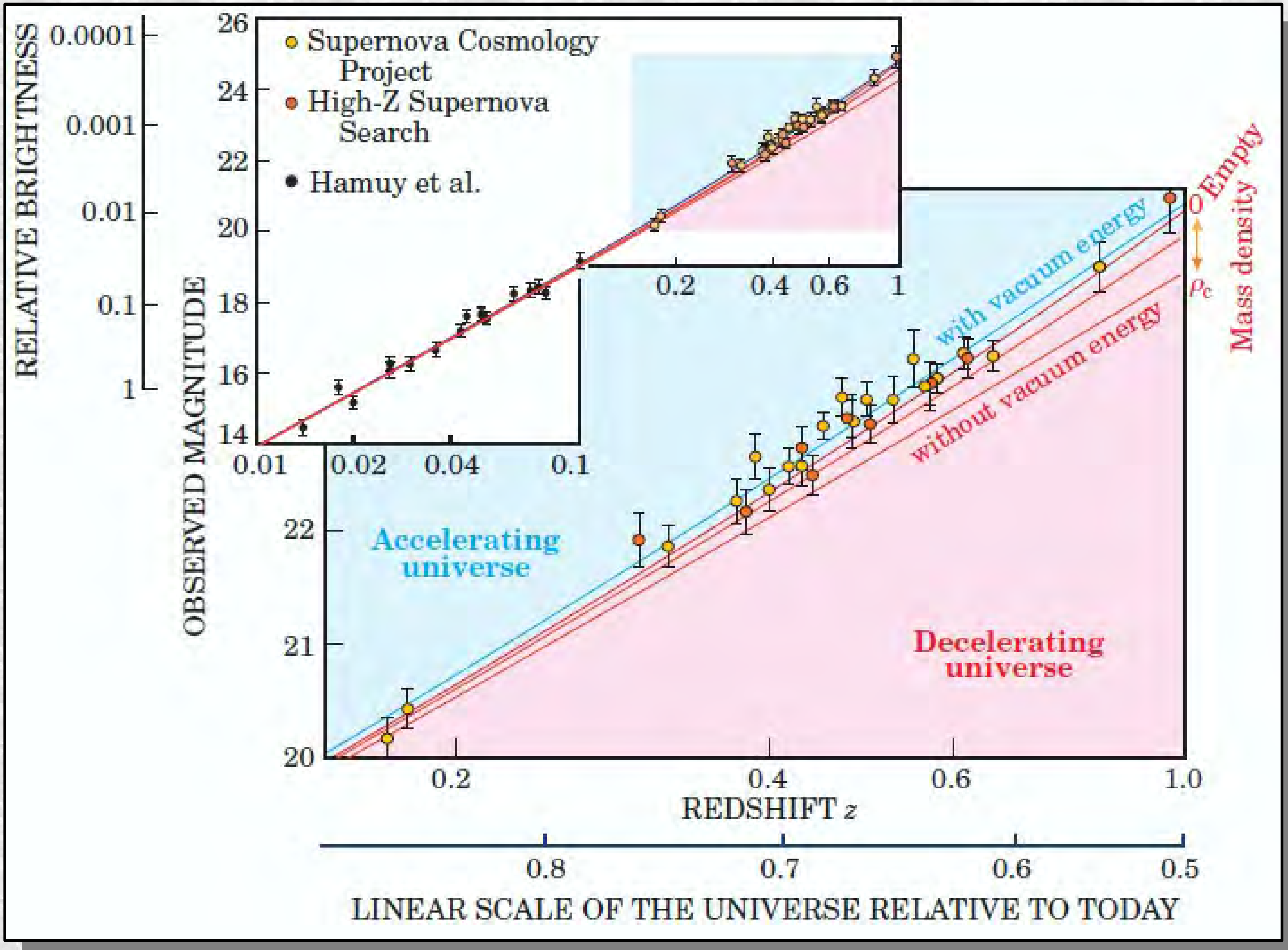

Source image : Physics Today, Avril 2003

Proc. Natl. Acad. Sci. USA
Vol. 96, pp. 4224–4227, April 1999

Perspective

Supernovae, an accelerating universe and the cosmological constant

Robert P. Kirshner

Harvard-Smithsonian Center for Astrophysics, 60 Garden Street, Cambridge, MA 02138

Observations of supernova explosions halfway back to the Big Bang give plausible evidence that the expansion of the universe has been accelerating since that epoch, approximately 8 billion years ago and suggest that energy associated with the vacuum itself may be responsible for the acceleration.

For 40 years, astronomers have hoped to measure changes in the expansion rate of the universe as a way to measure the mass density of the universe and the geometry of space and to predict the future of cosmic expansion. In 1998, two groups reported plausible evidence based on supernova explosions that the expansion of the universe is not slowing down, as predicted by the simplest models, but actually accelerating. If these results are confirmed, it will require a major change in our picture for the universe. We will be forced to add another constituent to our best model for the universe, a form of vacuum energy that drives the expansion, which makes the large-scale geometry Euclidean, and which contains most of the energy density in the universe (1). This paper aims to sketch the background to this discovery, to show some of the evidence for cosmic acceleration, and to equip an interested, but skeptical, reader with the right kinds of questions to ask of astrophysical colleagues.

Astronomers have known since Hubble's observations in 1929 that the universe is expanding (2). This was promptly incorporated into a dynamical picture of the universe based on general relativity, which describes how the presence of matter, or other energy forms in the universe, affect the curvature of space and the expansion of the universe. A decade before the discovery of cosmic expansion, Einstein introduced a "cosmological constant" into his equations, to make the universe static, in accord with the astronomical wisdom of the day. When the astronomical evidence changed, he quickly abandoned the cosmological constant and much later referred to it as his "greatest blunder" (3). Since 1929, it has been the burning ambition of observers of the expanding universe to determine the energy content and the curvature from astronomical measurements. In 1998, we may have achieved that long-sought-after goal.

The observational problem is to discover objects that can be seen at large redshifts, so the cosmological effects are large enough to measure, and that are well enough understood so that their apparent brightness can be trusted to give a reliable measure of their distance. The long, winding path of observational cosmology is littered with the wreckage of past attempts to do this with galaxies, whose properties evolve over time much too rapidly to serve as "standard candles" for this work. But type Ia supernovae (SN Ia) can be seen to redshift 1, and their intrinsic scatter in brightness is small enough so that the cosmological effects on the observed brightness as a function of redshift can be measured. At a redshift of 0.5, the difference in apparent magnitude between a universe that is flat, decelerating, and just barely closed by matter, $\Omega_m = 1$, and a universe that is hyperbolic and empty, $\Omega_m = 0$, is $\approx$25% in the flux of a supernova. The scatter in SN Ia brightness for a single object, after correcting for the light curve shape (as described below), is only $\approx$15%, so a relatively small number of supernovae can produce a significant measurement of the cosmology. The result is surprising evidence for an accelerating, but geometrically flat, universe.

FIG. 1. SN 1994D, a nearby supernova imaged with the Hubble Space Telescope.

The Brightest Supernovae

Supernovae were named and classified by the astrophysicist Fritz Zwicky in the 1930s. They are powerful stellar explosions in which a single star becomes as bright as 10^9 stars like the sun. The modern taxonomy of supernovae (4) separates them into two types, type I (SN I) and type II (SN II) depending on whether they show hydrogen lines in their spectra at maximum light. A more physical description, based on models for the explosions and circumstantial evidence based on the locations where supernovae of various types are found, attributes the hydrogen-free type Ia supernovae to the thermonuclear detonation of white dwarf stars and the type II (as well as SN Ib and Ic) to the core collapse of massive stars. The SN Ia are thought to leave no stellar remnant while the SN II and their cousins are responsible for the formation of neutron stars and stellar-mass black holes. Despite their very different origins and mechanisms, the intrinsic luminosity of both types is comparable. The combined rates of supernovae are on the order of a few per century in a galaxy like ours. Tycho's supernova of 1572, in our own Milky Way, was probably a SN Ia, while SN 1987A in the Large Magellanic Cloud was a variant of the SN II class.

For cosmology, the key property that makes SN Ia useful is that they are the brightest class of supernova and have the smallest spread in intrinsic luminosity. Theoretically, a narrow range of

PNAS is available online at www.pnas.org.

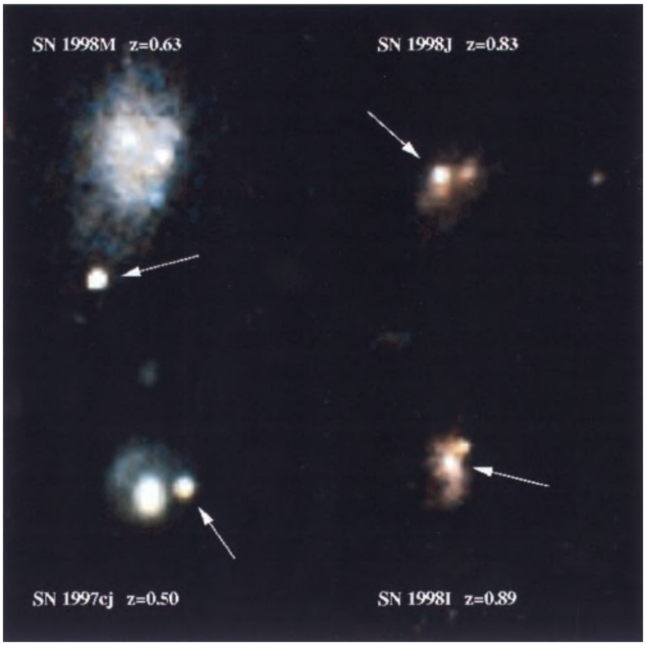

FIG. 2. High redshift supernovae observed with the Hubble Space Telescope.

luminosities for SN Ia might stem from the upper mass limit for the white dwarfs that explode to form them: 1.4 solar masses is the Chandrasekhar limit for electron degeneracy support of a cold mass of carbon and oxygen that comprises a white dwarf. Though a carbon-oxygen white dwarf at the Chandrasekhar limit is stable, it may explode if a binary companion adds to its mass. When a thermonuclear burning wave destroys such a star, by burning approximately 0.5 solar mass of it to iron-peak elements, the resulting "standard bomb" may make a good beacon to judge cosmic distances.

In the 1960s and 1970s, the measurements of supernova light curves were crude by modern standards because they were made with photographic plates, and it was plausible that all of the observed variation in SN Ia luminosities came from the difficult problem of measuring the supernova light on the background of a distant galaxy with a nonlinear detector (Fig. 1). In that innocent time, imaginative theorists (for example, see refs. 5 and 6) sketched how supernova observations might be used to determine whether the universe was decelerating, as would be expected if gravity's effect had been accumulating over the time of cosmic expansion, by looking at the redshifts and fluxes for distant supernovae.

Search for the 'Standard Bomb'

The advent of charge-coupled device (CCD) silicon detector arrays made it possible to find supernovae that are far enough away for deceleration to produce a measurable deviation from the inverse square law seen by Hubble. The observational problem was to find these faint and distant supernovae near the peak of their light curves. This challenge was met by a Danish-led group (7) who anticipated most of the techniques used later. They made monthly observations at the Danish 1.5-m telescope in Chile to catch fresh supernova explosions and used a CCD to gather their data and a computer to subtract a reference image from each night's picture to find the new events. They coordinated follow-up observations to get spectra (to show the events were really SN Ia and to get the redshift) and to measure the light curve of the supernova's rise and fall. However, in 2 years of searching, because their small telescope was slow to reach faint magnitudes and their CCD had a small field of view, they only snared one good event, SN 1998U, which was a SN Ia at a redshift of 0.3, and then retired from the field.

The widespread application of CCDs and a diligent attention to studying all of the bright supernovae soon made it clear that there were real differences in intrinsic brightness among SN Ia. In 1991 alone, the observed range in brightness, from SN 1991bg to SN 1991T, was approximately a factor of 3. Left untreated, this scatter could wreak havoc with attempts to judge cosmic acceleration. Determining the relation between distance and redshift through a standard candle only works well when the distance can be inferred precisely from the flux. While some brave souls forged ahead with further attempts to find distant supernovae by extending the methods of the Danes to bigger, faster telescopes and more capable detectors provided at the U.S. National Optical Astronomy Observatories (8), a group of astronomers at the University of Chile's Cerro Calán observatory and their partners at the Cerro Tololo Interamerican Observatory (CTIO) began the Calán/Tololo supernova search (9) to strengthen our understanding of SN Ia as distance indicators.

Although the Calán/Tololo search was carried out photographically, this was very effective in searching wide areas of the sky for nearby supernovae. Because the astronomers could be certain that each month's search would have a good probability of turning up one or more SN Ia, they were able to schedule follow-up observations with the CTIO telescopes to obtain good CCD observations of their discoveries. Following the clues derived earlier from a few objects (10), the Calán/Tololo measurements showed that, although there was a real variation in the luminosity of SN Ia, it was closely correlated with the shape of the supernova's light curve. Intrinsically luminous supernovae rise slowly and decline slowly, while their fainter siblings rise and decline more quickly (11). More SN Ia light curves were added to the database (12, 13) and a more sophisticated way to use all the information in the light curve to estimate the distance, the

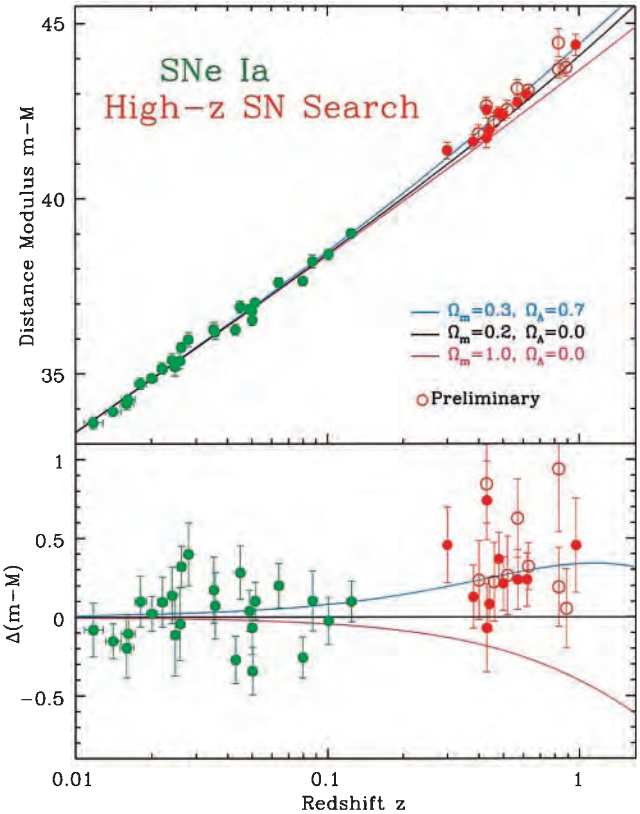

FIG. 3. The Hubble diagram for SN Ia. The lines show the predictions for cosmologies with varying amounts of Ω_m and Ω_Λ. The observed points all lie above the line for a universe with zero Λ. The lower panel, with the slope caused by the inverse square law taken out, shows the difference between the predictions more clearly and shows why a model with $\Omega_\Lambda > 0$ is favored.

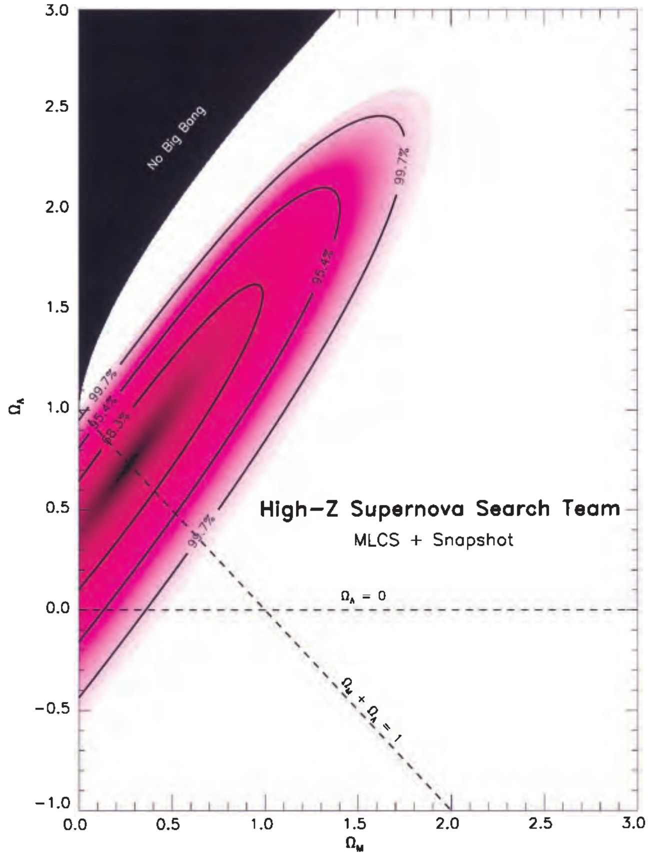

FIG. 4. The Ω_m, Ω_Λ plane. Using the supernova data, a likelihood analysis shows the probability that any chosen pair of Ω_m, Ω_Λ values fits the observations. The allowed region is large and follows the direction of $\Omega_m - \Omega_\Lambda$ = a constant. $\Omega_m = 1$ is far from the allowed region. Many pairs of geometrically flat solutions with $\Omega_m + \Omega_\Lambda = 1$ are possible. $\Omega_\Lambda = 0$ is not very probable in this analysis.

Multicolor Light Curve Shape method (MLCS), was created (12, 13). As a result of these efforts, the scatter in luminosity for SN Ia was pushed downward from approximately 40% to less than 15%, which makes SN Ia the best standard candles in astronomy and suitable tools for the fine discrimination needed to discriminate one history of the universe from another.

Meanwhile, the Supernova Cosmology Project (SCP) continued to search for high redshift supernovae. By 1997, the SCP had a preliminary result (14). Based on seven supernovae discovered in 1994 and 1995, the Calán/Tololo low redshift sample, and a variant of the luminosity-light curve relation, they concluded that the evidence favored a high matter density universe, $\Omega_m = 0.88 \pm 0.6$. They argued that the supernova data at that point placed the strongest constraint on the possible value of the cosmological constant, with their best estimate being $\Omega_\Lambda = 0.05$.

Another group, the High-Z Supernova Team (of which I am a member) introduced a number of new developments, including custom filters, which help minimize the effect of redshift on interpreting the observed fluxes, and ways to use observations in two colors to estimate the absorbing effects of interstellar dust on the supernova light by measuring the reddening it produces. The High-Z team found its first supernova, SN 1995K, in 1995 (15) and now has detected more than 70 events. Fig. 2 illustrates some of the high redshift supernovae discovered by the High-Z Team that have been observed with the Hubble Space Telescope (HST). The supernovae are, in general, found and studied from ground-based observatories, but the HST provides much better separation of the supernova from the background galaxy, which leads to more precise measurements of the supernova's light curve.

Cosmic Acceleration

In 1998, both teams reported new results (15–20). As illustrated in Fig. 3, the Hubble diagram for SN Ia now extends to sufficiently high redshift and has enough supernovae with small enough error bars so that the expected effects of cosmic deceleration should be detectable. If the universe had been decelerating––in the way it would if it contained the closure density of matter, that is, if $\Omega_m = 1$—then the light emitted at redshift $z = 0.5$ by a SN Ia would not have traveled as far, compared with a situation where the universe had been coasting at a constant rate—characteristic of an empty universe, where $\Omega_m = 0$. For a universe with $\Omega_m = 1$, the flux from the distant supernova therefore would be ≈25% brighter. But the distant supernovae are not brighter than expected in a coasting universe, they are dimmer. For this to happen, the universe must be accelerating while the light from the supernova is in transit to our observatories.

Cosmic acceleration is not a new idea (21) and an energy component to the universe that might have an accelerating effect was proposed by Einstein in 1917. Since then, the cosmological constant has been like a pair of your grandfather's spats—occasionally tried on for costume events—but these new results suggest that they are not just coming back into fashion, they are now *de rigeur*.

The supernova results define an allowed region in the Ω_m, Ω_Λ plane, as shown in Fig. 4. The constraint is approximately described by $\Omega_m - \Omega_\Lambda$ = constant, which gives a surprisingly tight limit on the expansion time, which for a plausible Hubble constant of 65 km $\sec^{-1}\cdot\mathrm{Mpc}^{-1}$ is 14 ± 1 Gyr. Although a matter-dominated universe with $\Omega_m = 1$ appears to be ruled out by the data, and on the face of it $\Omega_\Lambda > 0$ is favored by the supernova observations, there is still a remote possibility that the present observations can be produced in a universe where the cosmological constant is 0. However, as both teams build up the data and improve their understanding of possible systematic effects, that faint hope for a simpler universe could be snuffed out.

An interesting exercise is to combine the supernova data with measurements of the fluctuations in the cosmic microwave background (CMB). Present-day observations suggest there is a characteristic angular scale to the CMB roughness around the 1° scale that can be linked through robust theory to the linear scale of fluctuations at the time when the universe became transparent. This translates into a constraint on $\Omega_m + \Omega_\Lambda$, which many theorists have noticed is orthogonal to the supernova constraint. By combining the two types of measurements, it has been shown that the best solution for the High-Z sample (shown in Fig. 5) has $\Omega_m = 0.3$ and $\Omega_\Lambda = 0.7$ (19). This is a plausible pair of values. The matter density has been estimated by several routes (which have nothing to do with supernovae or the CMB) to be in the vicinity of $\Omega_m = 0.3$, while a universe in which $\Omega_m + \Omega_\Lambda = 1$ gives the universe the geometry of flat space and often is cited as a prediction of the simplest models of inflationary cosmology. The CMB results will continue to improve as the results flow in from a large number of ground- and balloon-based experiments. Decisive results from the Microwave Anisotropy Probe satellite are expected in 2002.

Problems with the SN Ruler?

It is still early days in the use of high redshift supernovae for cosmology. Could there be some problem with the use of SN Ia that has not yet come to light? Could there be some other reason, which has nothing to do with cosmology, that makes the objects found at a redshift $z = 0.5$ approximately 25% fainter than the SN Ia we see nearby? While both teams have tried hard to identify and rule out systematic problems, both are using a slender (and common) database of local supernovae to correct the observed fluxes for the effects of the supernova redshift and spectral details as observed through fixed filters. These "k-corrections" conceivably could produce some problems for particular supernova ages and redshifts, but because the supernovae are sampled over a significant range of redshifts and through a variety of filters, it is hard to see exactly how this technical detail would produce the

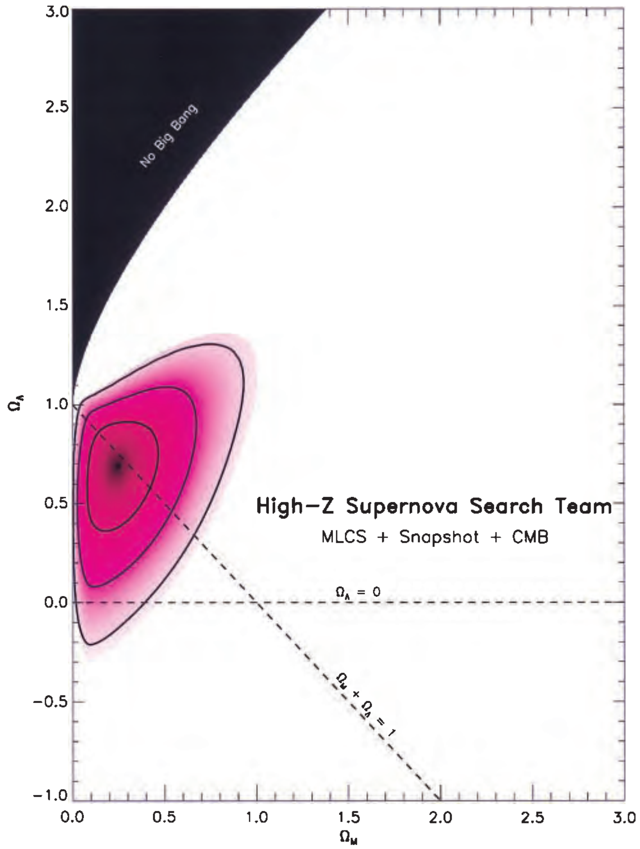

FIG. 5. Ω_m, Ω_Λ plane for the combination of supernova constraints and measurements of the CMB.

observed effect. Still, it will be well worth the trouble to gather detailed observations of nearby supernovae as they are discovered to improve our knowledge of supernova spectra.

It is not hard to imagine other possibilities that could lead to problems based on the supernovae themselves: the distant supernovae are explosions that took place 8 billion years ago. They are younger objects than nearby SN Ia. This could affect the properties of the stars that led to SN Ia long ago compared with the present and also could affect the chemical composition of the white dwarfs that explode, both near and far. Because the present-day understanding of SN Ia is incomplete, we don't know exactly how changes in the stellar population or the composition would affect the luminosity (22). However, the evidence from nearby samples with different star-forming histories, in spiral and elliptical galaxies, is that the light curve shape methods account for the systematic difference between SN Ia in old and young stellar populations.

Even more sinister could be the effects of cosmic dust, which could absorb light from distant supernovae, and lead to their apparent faintness. However the interstellar dust in our own galaxy absorbs more blue light than red, so it leaves a distinct reddening signature that the two-filter observations should detect. The High-Z Team corrects for both the nearby and distant supernovae in the same way by using these color measurements, which should eliminate the effects of interstellar dust from Fig. 3. The Supernova Cosmology Project argues that the dust effect is small and similar in the high and low redshift samples, so no net correction is needed. It is possible to imagine special dust that is not noticed nearby and that has the right size distribution to absorb all wavelengths equally (23). Such "gray dust" would have to be smoothly distributed, because we do not see the increased scatter that patchy dust thick enough to produce the observed dimming, would introduce. If this material exists, there is a powerful test that could discriminate between a cosmology that is dominated by Ω_Λ and one in which specially constructed dust produces the dimming at redshift 0.5. Since a cosmological constant is a constant energy density, while the density of matter has been declining as $(1+z)^3$, by looking back to $z = 1$, we could observe the era (not so long ago) when matter was the most important constituent of the universe and the universe was decelerating. At those redshifts, the relation between redshift and flux would bend back toward brighter fluxes, while the effects of gray dust presumably would grow, or at least remain constant. To make accurate measurements of this effect will require discovering and making good measurements of redshift 1 supernovae whose light is redshifted into the infrared. The Next Generation Space Telescope may play an important role in this decisive test.

Finally, I note that a constant energy density is not the only possibility. More elaborate physical models in which the energy density changes with time also have been proposed (24), and they can be constrained by using the supernovae and other observations. But in any case, it seems as if supernova observations finally have made it possible to carry out the program outlined by Sandage (25, 26) to determine the acceleration and the geometry of the universe by observing the distances and redshifts of standard candles.

1. Hogan, C. J., Kirshner, R. P. & Suntzeff, N. B. (1999) *Sci. Am* **280,** 28–33.
2. Hubble, E. P. (1929) *Proc. Natl. Acad. Sci. USA* **15,** 168.
3. Goldsmith, D. (1995) *Einstein's Greatest Blunder?* (Harvard Univ. Press, Cambridge, MA).
4. Filippenko, A. V. (1997) *Annu. Rev. Astron. Astrophys.* **35,** 309–355.
5. Wagoner, R. V. (1977) *Astrophys. J. Lett.* **214,** L5–L7.
6. Colgate, S. A. (1979) *Astrophys. J.* **232,** 404–408.
7. Norgaard-Nielsen, H. U., Hansen, L., Jorgensen, H. E., Salamanca, A. A., Ellis, R. & Couch, W. J. (1989) *Nature (London)* **339,** 532–534.
8. Perlmutter, S., Pennypacker, C. R., Goldhaber, G., Goobar, A., Muller, R. A., Newberg, H. J. M., Desai, J., Kim, A. G., Kim, M. Y., Small, I. A., *et al*. (1995) *Astrophys. J. Lett.* **440,** L41–L44.
9. Hamuy, M., Maza, J., Phillips, M. M., Suntzeff, N. B., Wischnjewsky, M., Smith, R. C., Antezana, R., Wells, L. A., Gonzalez, L. E., Gigoux, P., *et al*. (1993) *Astronom. J.* **106,** 2392–2407.
10. Phillips, M. M. (1993) *Astrophys. J. Lett.* **413,** L105–L108.
11. Hamuy, M., Phillips, M. M., Suntzeff, N. B., Schommer, R. A., Maza, J., Smith, R. C., Lira, P. & Aviles, R. (1996) *Astronom. J.* **112,** 2438–2447.
12. Riess, A. G., Press, W. H. & Kirshner, R. P. (1995) *Astrophys. J. Lett.* **439,** L17–L20.
13. Riess, A. G., Press, W. H. & Kirshner, R. P. (1996) *Astrophys. J.* **473,** 88–109.
14. Perlmutter, S., Gabi, S., Goldhaber, G., Goobar, A., Groom, D. E., Hook, I. M., Kim, A. G., Kim, M. Y., Lee, J. C., Pain, R., *et al.* (1997) *Astrophys. J.* **483,** 565–568.
15. Schmidt, B. P., Suntzeff, N. B., Phillips, M. M., Schommer, R. A., Clocchiatti, A., Kirshner, R. P., Garnavich, P. M., Challis, P., Leibundgut, B., Spyromilio, J., *et al.* (1998) *Astrophys. J.* **507,** 46–63.
16. Perlmutter, S., Aldering, G., Della Valle, M., Deustua, S., Ellis, R. S., Fabbro, S., Fruchter, A., Goldhaber, G., Groom, D. E. & Hook, I. M. (1998) *Nature (London)* **391,** 51–54.
17. Perlmutter, S., Aldering, G., Goldhaber, G., Knop, R. A., Nugent, P., Castro, P. G., Deustua, S., Fabbro, S., Goobar, A., Groom, D. E., *et al.* (1999) *Astrophys. J.*, in press, astro-ph/9812133.
18. Garnavich, P. M., Kirshner, R. P., Challis, P., Tonry, J., Gilliland, R. L., Smith, R. C., Clocchiatti, A., Diercks, A., Filippenko, A. V., Hamuy, M., *et al.* (1998) *Astrophys. J. Lett.* **493,** L53–L57.
19. Garnavich, P. M., Jha, S., Challis, P., Clocchiatti, A., Diercks, A., Filippenko, A. V., Gilliland, R. L., Hogan, C. J., Kirshner, R. P., Leibundgut, B., *et al.* (1998) *Astrophys. J.* **509,** 74–79.
20. Riess, A. G., Filippenko, A. V., Challis, P., Clocchiati, A., Diercks, A., Garnavich, P. M., Gilliland, R. L., Hogan, C. J., Jha, S., Kirshner, R. P., *et al.* (1998) *Astrophys. J.* **116,** 1009–1038.
21. Carroll, S. Press, W. H. & Turner, E. L. (1992) *Annu. Rev. Astron. Astrophys.* **30,** 499–542.
22. Hoeflich, P., Wheeler, J. C. & Thielemann, F. K. (1998) *Astrophys. J.* **495,** 617–629.
23. Aguirre, A. (1999) *Astrophys. J.,* in press, astro-ph/ 9811316.
24. Caldwell, R. R., Dave, R. & Steinhardt, P. J. (1998) *Phys. Rev. Lett.* **80,** 1582–1588.
25. Sandage, A. R. (1961) *Astrophys. J.* **133,** 355–392.
26. Sandage, A. (1988) *Annu. Rev. Astron. Astrophys.* **26,** 561–630.